Use of Microstrip Impedance-Measurement Technique in the Design of a BARITT Diplex Doppler Sensor

B. MERVYN ARMSTRONG, MEMBER, IEEE, ROBERT BROWN, FRED RIX, AND J. A. CARSON STEWART

Abstract—**A computer-aided microstrip impedance-measurement technique, which yields information on microstrip-material properties, is described. The technique is used to investigate the impedance of microstrip-mounted BARITT diodes and of microstrip pad antennas. A Doppler sensor is designed, incorporating the BARITT diode into a microstrip circuit, and used in a diplex Doppler range-measuring radar.**

I. Introduction

STANDARD short-range Doppler radars provide information on target speed relative to the radar. In certain applications, e.g., vehicle sensing, instantaneous target range and sense of direction are required. By using the diplex mode of operation [1] and by incorporating a BARITT diode as a self-oscillating mixer into a microstrip circuit, a Doppler sensor module has been developed which combines small size with moving-target range and direction-sense output. The sensor (Fig. 1) is a packaged BARITT diode mounted in a microstrip circuit. The circuit, consisting of pad antenna, bias pad and filter, and matching stub, is patterned on RT/Duriod 5880 microstrip material. The design of the sensor is based on a computer-controlled system, which enables accurate measurement of impedance on the microstrip to be performed.

This paper describes the microstrip measurement system and typical results thereof. The measured BARITT-diode impedance is then used to justify the system accuracy and to provide data for the sensor design. Measurements of pad-antenna input impedance are described, are compared with simple theory, and are then used in conjunction with the diode impedance in the design of the sensor. The final section discusses the operation of a diplex-radar system incorporating the microstrip sensor.

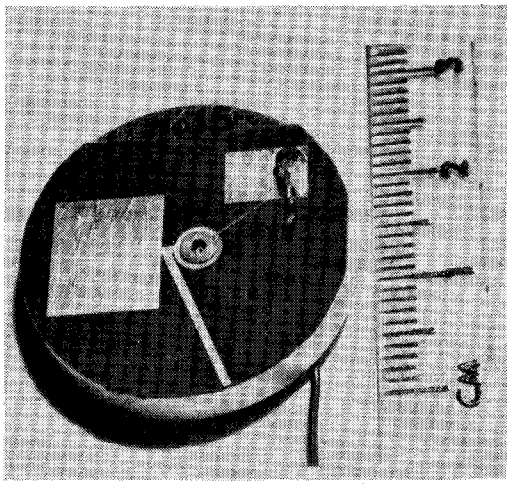

Fig. 1. BARITT-diode microstrip Doppler sensor.

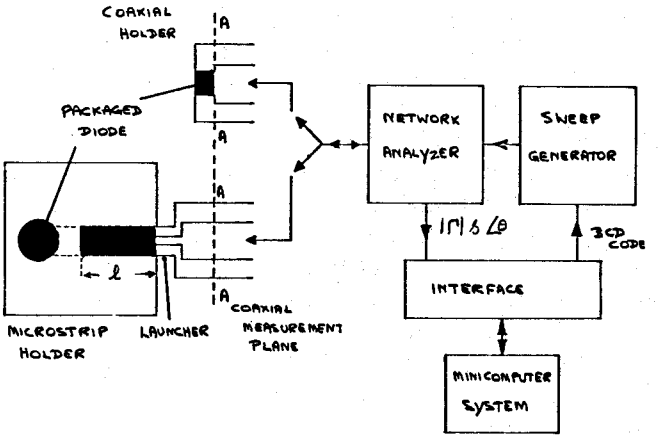

Fig. 2. Microstrip impedance-measuring system.

II. Microstrip Measurement System

Fig. 2 shows the layout of the impedance-measurement system. The network analyzer and the sweep generator are standard units, producing an output corresponding to the magnitude and phase of the reflection coefficient at plane *A–A*, over the frequency range of 8–12.4 GHz. The minicomputer is CA LSI-2 model, with a dual floppy-disk drive and 32K words of storage. The interface unit transmits the appropriate BCD code from the computer to the sweep generator, producing the required frequency sequences within the system operating range, and receiving analog signals ($|\Gamma|$ and θ) from the network analyzer. These are digitized and fed to the minicomputer for signal processing. The active device, e.g., the BARITT diode, can be placed into a coaxial holder, from which the chip impedance and the package and mount equivalent circuits can be determined from impedance measurements at the

Manuscript received May 21, 1980; revised August 4, 1980. Part of the work described in this paper was supported by the Science Research Council, England.

The authors are with the Department of Electrical and Electronic Engineering, Ashby Building, The Queen's University of Belfast, Northern Ireland, U.K.

0018-9480/80/1200-1437$00.75 ©1980 IEEE

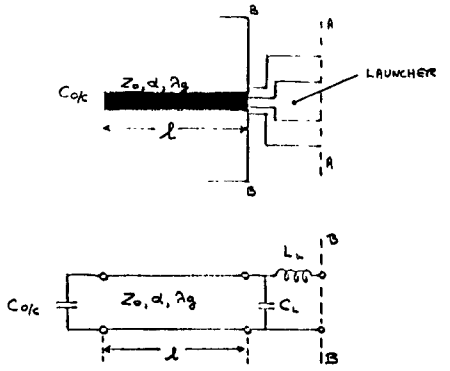

(a)

FREQ. (GHz)	ϵ_{eff}	$C_{o/c}$ (pF)	C_L (pF)	L_L (nH)	α (dB/cm)	Z_0 (Ω)	ERROR θ	ERROR |Γ|
9.5-10.0	1.837	0.047	0.088	0.646	0.038	66.2	0.237	0.006
10.0-10.5	1.836	0.047	0.088	0.651	0.062	62.1	0.23	0.002
10.5-11.0	1.832	0.046	0.093	0.663	0.073	60.58	0.294	0.003
11.0-11.5	1.827	0.048	0.094	0.644	0.093	61.55	0.352	0.005

(b)

Fig. 3. (a) Open-circuited microstrip line and launcher equivalent circuit. (b) Typical experimental results.

plane A–A. The reach-through capacitance of the BARITT measured at 1 MHz is used as a reference, and a computer minimization program finds values for the equivalent circuit.

For microstrip measurements, an OSM 244-4A launcher is used to transform from precision 50-Ω coaxial line to planar microstrip. The unit under test is connected to the launcher through a length of microstrip line. In order to find the unknown impedance, the launcher transformation and microstrip line parameters (characteristic impedance Z_0, wavelength λ_g, and attenuation α) must be determined. The method used is an extension of that suggested by Wight *et al.* [2]. Fig. 3(a) shows one equivalent circuit for an open-circuit length of microstrip line, connected to the B–B plane via a launcher. The launcher is represented by a simple L–C equivalent circuit. The line attenuation is expressed in dB/cm. λ_g, the wavelength in the microstrip line, is related to the effective dielectric constant ϵ_{eff}, by

$$\lambda_g = \frac{c}{f\sqrt{\epsilon_{ff}}}.$$

A launcher, short-circuited at the "beak," is used as the reference short circuit when setting up the network analyzer, thus reducing the effect of the necessary APC-7 to OSM transformer. Any subsequent field irregularity in transforming from coaxial to microstrip geometry is accounted for by L_L and C_L. The method of measurement proceeds as follows:

a) Measure the input impedance of the active or passive circuit under consideration, at the short-circuited launcher reference plane.

b) Cut back the connecting microstrip line to create the open-circuited line of Fig. 3(a).

c) Measure the input impedance of the open-circuited line/launcher combination, either as a function of line length l at a fixed frequency, or as a function of frequency at a fixed line length. As the microstrip attenuation is a function of frequency, relatively limited frequency ranges should be used.

d) The computer minimization routine adjusts the element values of the equivalent circuit of Fig. 3(a), to minimize the errors between measured and calculated input impedance. In this procedure the error function is

$$F = \alpha_s \sum_i \{\mathrm{Re}(\Gamma_i^c) - \mathrm{Re}(\Gamma_i^m)\}^2 + \beta_s \sum_i \{\mathrm{Im}(\Gamma_i^c) - \mathrm{Im}(\Gamma_i^m)\}^2$$

where $\mathrm{Re}(\Gamma)$ and $\mathrm{Im}(\Gamma)$ are the real and imaginary parts of the reflection coefficient, and α_s and β_s are scaling factors. The superscripts, c and m, refer to calculated and measured values, respectively.

The table of Fig. 3(b) shows results from a characterization measurement performed with an open-circuited line length of 1.24 cm. The frequency has been varied over 500 MHz for several center frequencies. As the measurement wavelength increases, the input reflection-coefficient variation with frequency is reduced, producing an increased measurement error. The value of 1.836 for ϵ_{eff} and the line impedance of 61.5 Ω correspond to a material dielectric constant of 2.2, well within the laminate specifications. The equivalent circuit values are reasonably constant, with the expected exception of α, which increases with increasing frequency.

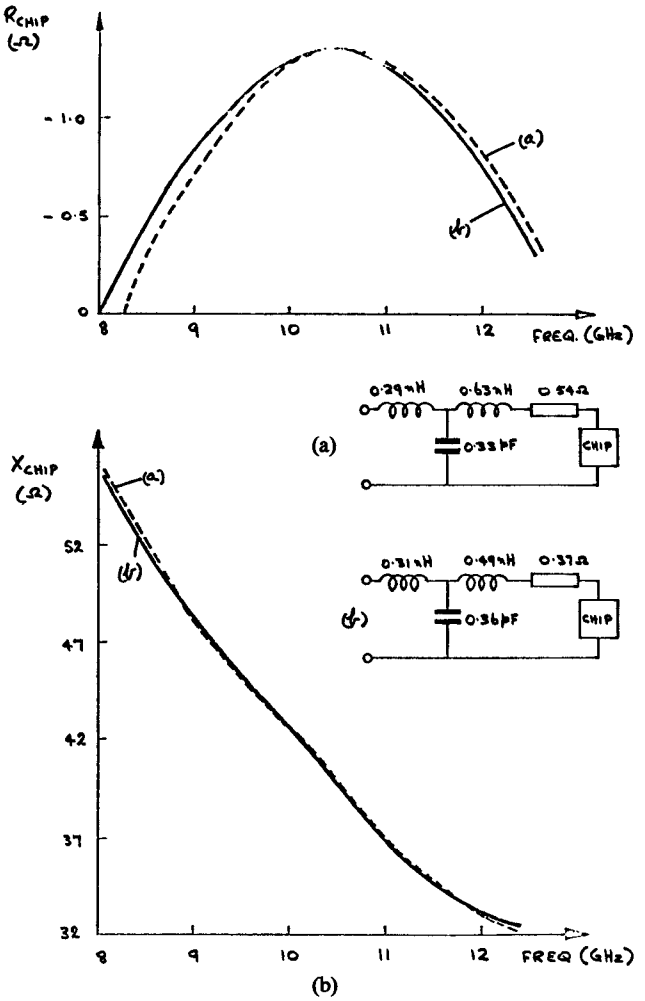

Fig. 4. BARITT chip impedance versus frequency at bias current of 5 mA. (a) Mount and package equivalent circuit, and chip impedance—one bonding lead. (b) Mount and package equivalent circuit, and chip impedance—two bonding leads.

The low average measurement errors in Fig. 3(b) indicate that the derived equivalent circuits can be used to transform the input impedances of section a) above, from the launcher plane to that of the unknown element. The following sections illustrate the use of this procedure in the measurement of BARITT-diode and pad-antenna input impedances.

III. BARITT-Diode Measurement

Two types of BARITT diode, fabricated within the department, have been used in the microstrip sensor:

a) p^+-n-p^+ diodes having an active length of 4.2×10^{-4} cm; n-region doping density of 2.5×10^{15} cm^{-3}; and areas of 1.2×10^{-4} cm^2, 1.6×10^{-4} cm^2, and 2.0×10^{-4} cm^2, and b) p^+-n-ν-p^+ diodes having the same basic structure as the p^+-n-p^+ devices, but with the addition of a phosphorous implant at a concentration 3.7×10^{11} cm^{-2} and an implant energy of 600 kV. The sensor will operate equally as well with either diode type. The operating bias for these devices is approximately 45 V at 5 to 15 mA dc.

Standard chip, package, and mount characterization is performed using the coaxial holder of Fig. 2. Using the measured chip capacitance at reach-through as reference, the minimization routine calculated equivalent circuit values as shown in Fig. 4. In Fig. 4, the impedance of a p^+-n-p^+ BARITT-diode chip at a dc bias current of 5 mA is plotted as a function of frequency. The impedance is derived from measurements on two separate packaged diodes (of the same type and with the same parameters). In case (a) the package has one bonding lead, while in case (b) two bonding leads are used. The close agreement between the chip impedances evaluated from the two measurements tends to validate the minimization procedure. Additionally, the reduction in the package lead inductance and the package series resistance when two leads are incorporated is as anticipated.

Accurate measurement of the input impedance in microstrip at the perimeter of the diode package is required for the overall sensor design. The equivalent circuit for the launcher and connecting microstrip line is found as dis-

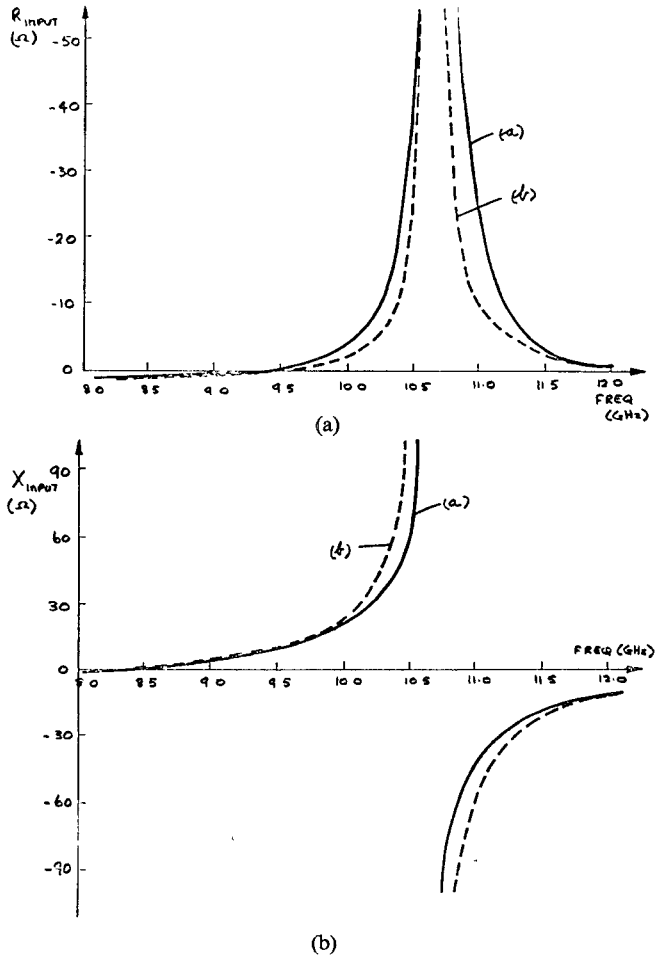

Fig. 5. Microstrip-mounted BARITT-package input impedance. (a) Computer simulation. (b) Measured using the minimisation procedure.

cussed above, and the active device impedance computed. The input-impedance variation with frequency for a p^+-n-p BARITT diode, having an area of 1.6×10^{-4} cm^2, at a dc bias current of 5 mA, is given in Fig. 5(b). Note the dominant mount parallel resonance at approximately 10.5 GHz. This resonant frequency can be varied a) by using diodes of different area, b) by using a different number of bond leads, c) by changing the diameter of the radial ring used to facilitate contract between the diode package and the microstrip circuit, or d) by operating at different bias currents.

In order to verify the measurement, a further minimization was used to determine the equivalent-circuit values for the microstrip-mounted diode, shown in Fig. 6. This circuit was used in conjunction with the measured input impedance of Fig. 5(b) to evolve the chip impedance. In Fig. 6, the chip impedance is compared with that of the same diode measured in the coaxial holder. The agreement is acceptable. Note that the equivalent-circuit values for the microstrip-mounted package differ markedly from those of the coaxial-mounted package, due to the slight increase in package inductance caused by recessing into the microstrip holder, and the increase in package capacitance accentuated by the radial contact ring.

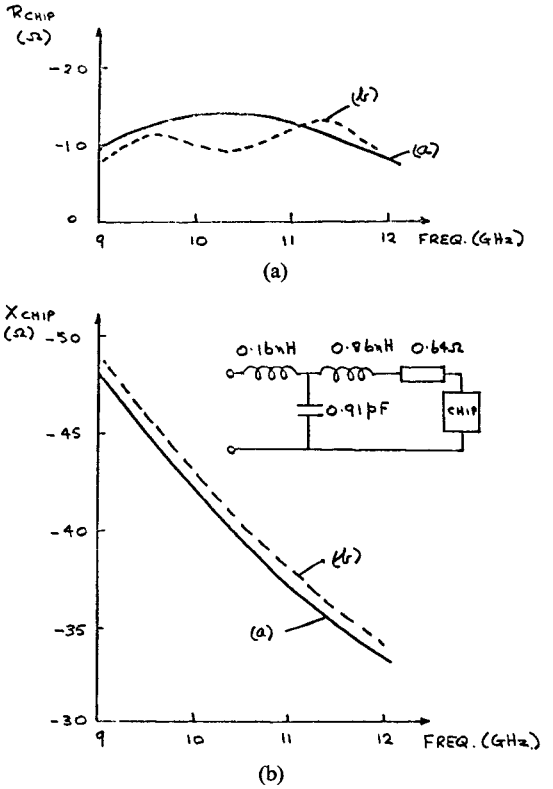

Fig. 6. BARITT-chip impedance as a function of frequency, evaluated (a) using a coaxial mount, (b) using a microstrip mount.

Further justification of the microstrip measurement is provided by a small-signal computer-simulation program, which for a p^+-n-p BARITT diode with appropriate physical parameters, and the package and mount equivalent circuit values of Fig. 6, predicted the microstrip input impedance variation with frequency as shown in Fig. 5(a).

IV. Pad-Antenna Measurement

Initial design of the simple rectangular pad antenna, is based on the equations given by Bahl [3]

$$a=\frac{\lambda_0}{2\sqrt{\epsilon_{\text{eff}}}}-2\Delta l \qquad b=\frac{\lambda_0}{2}\cdot\frac{1}{\sqrt{\frac{\epsilon_r+1}{2}}}$$

where λ_0 is the free-space wavelength, ϵ_r is the laminate dielectric constant (2.2), ϵ_{eff} is the effective dielectric constant of pad line, and Δl the equivalent length of the capacitive discontinuity at the radiating edge. The pad-antenna line impedance is 5 Ω, for which $\epsilon_{\text{eff}}=2.14$, giving dimensions $a=0.93$ cm, $b=1.10$ cm for a center frequency of 10.7 GHz.

The measured input impedance versus frequency characteristics of several pad antennas designed to have center frequencies between 10.5 and 11 GHz are found to fit closely the template of Fig. 7 when scaled to f_0. However, in each case the center frequency is found to be approximately 50 MHz below the design value. In addition, the input resistance at resonance is approximately 250 Ω, compared with a theoretical estimate of 277 Ω for a pad

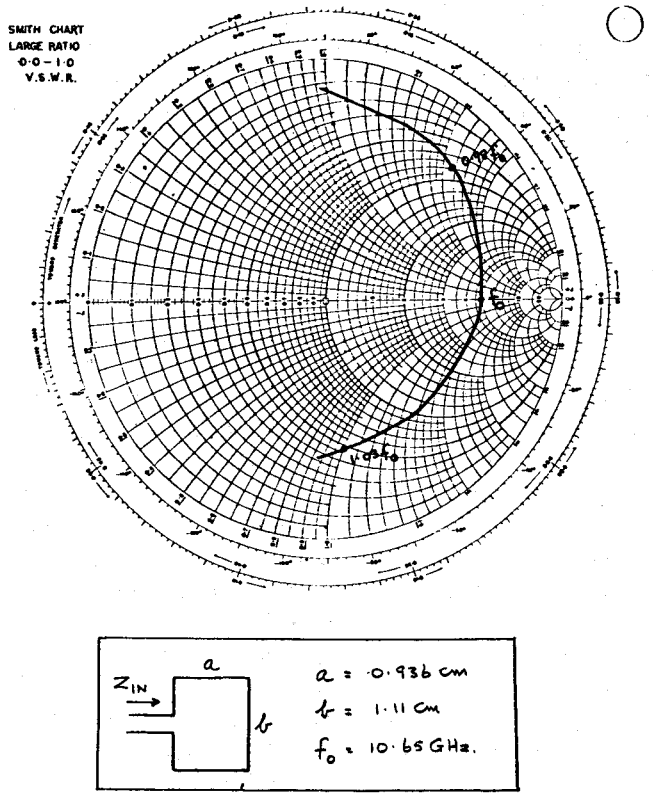

Fig. 7. Measured input impedance of rectangular pad microstrip antenna.

antenna with $b \simeq 0.4\lambda_0$ [3]. The discrepancies are thought to be due to slight dimensional inaccuracies in the final microstrip circuit. The measured dimensions of the nominal 10.7-GHz antenna are given in Fig. 7, and agree reasonably well with the measured center frequency of 10.65 GHz.

The theoretical gain of the pad antenna used in the sensor (10.65-GHz center frequency) is 7.3 dB, assuming 90-percent antenna efficiency.

V. Microstrip-Sensor Design

The sensor microstrip circuit of Fig. 1, based on impedance measurements of the packaged BARITT diode and pad antenna, is designed to provide a conjugate match at a center frequency of 10.65 GHz. The mount input impedance of an implanted diode (p^+-n-ν-p^+) of area 2×10^{-4} cm^2, operating at a bias current of 10 mA, is $-10+j30\ \Omega$ at 10.65 GHz (below the mount parallel resonance). An open-circuit shunt stub of 50-Ω nominal characteristic impedance and length 0.35 cm is used to transform the antenna input resistance of 250 Ω to the required load impedance of $5-j30\ \Omega$. A longer stub is used, which then is trimmed to facilitate tuning the output frequency of the module. The design is completed by a bias pad, which is isolated from the remainder of the circuit by a quarter-wave transformer.

In operation, the sensor output frequency can be changed from 10.1 to 10.8 GHz by varying the stub length from approximately zero to 0.5 cm. At stub lengths greater

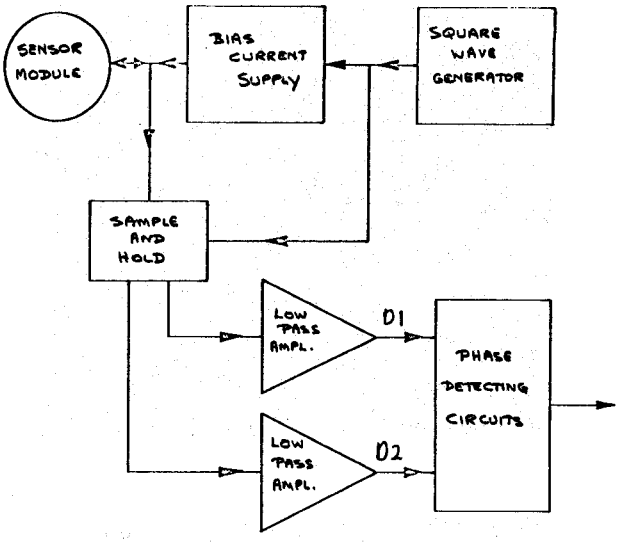

Fig. 8. Block diagram of diplex Doppler system.

than $0.5\lambda_g$ at the design frequency, an inductive reactance is presented to the BARITT-diode mount, causing a mode jump to a frequency above the parallel resonance frequency of approximately 12.2 GHz with a dramatic decrease in output power. At a dc bias current of 8 mA and with an antenna gain of 7.3 dB, the output power of the BARITT oscillator is estimated to be 0.4 mW. The radiated power density at 1 m from the sensor antenna is calculated to be 1.7×10^{-5} mW/cm^2. Using a spectrum analyzer, no spurious or harmonic output signals up to 40 GHz can be observed which are greater than -40 dBC.

VI. Diplex-Radar Performance

Fig. 8 is a block diagram of the diplex radar, which incorporates the sensor module. The transmitter is switched between two frequencies, 3 MHz apart, centered on the design frequency of 10.65 GHz. This provides a maximum unambiguous range of 25 m and a range resolution of approximately 0.5 m. The frequency switching is achieved by square-wave modulating the BARITT-diode bias current at a rate of 3 kHz, resulting in an output spectrum consisting of two discrete spectral lines separated by 3 MHz. The signal reflected from a moving target is incident on the oscillating BARITT diode. The resulting video output is a composite of two Doppler signals at approximately similar frequency but differing in phase, which are superimposed on the bias modulation waveform. By synchronously sampling the composite output signal in a sample-and-hold circuit, two separate chopped Doppler signals are recovered. These are smoothed in the low-pass amplifiers and then compared in the phase-detecting circuit. Fig. 9 shows the smoothed Doppler output signals ($D1$ and $D2$) (a) for a target approaching the radar and (b) for a receding target. The sign of the phase difference is a measure of the direction of the target motion, while the magnitude of the phase difference is proportional to the instantaneous target range.

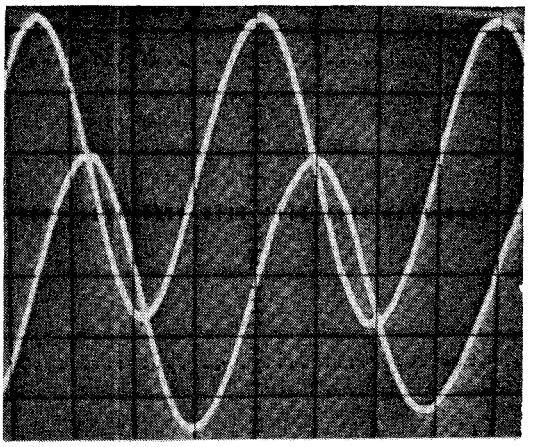

(a)

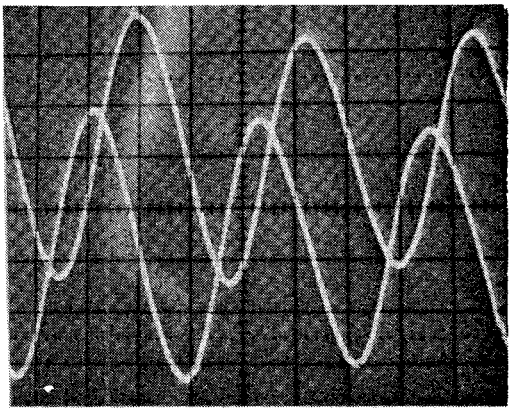

(b)

Fig. 9. Phase-detector output from diplex radar (a) with approaching target, (b) with receding target.

In laboratory tests, the radar sensitivity of the module has been measured to be −123 dBm/Hz at a Doppler frequency of 100 Hz, improving to −128 dBm/Hz at 1 kHz. For a human target, the maximum range is found to be 20 m with a video bandwidth of 100 Hz. For a small car at 10 mi/h the range increases to 35 m at a video bandwidth of 400 Hz. Assuming a target gain for the man of 40 dB and a transmitted power of −4.7 dBm, the radar equation predicts a receiver input power density of −120 dBm/Hz, which shows reasonable agreement with the measured sensitivity.

This performance is comparable to that reported for conventional, i.e., non-range-measuring, self-oscillating BARITT Doppler radars [4], [5].

VII. Conclusions

A computer-aided microstrip impedance-measurement system has been described. The measurement procedure yields information on microstrip-material properties, which are consistent with the manufacturers specifications.

The system has been used to measure the input-impedance variation with frequency of microstrip-mounted BARITT diodes and of microstrip pad antennas. Estimates of the BARITT-diode chip impedance, which are derived from input-impedance measurements have been used to validate the system and the measurement procedure.

Finally, the performance of a Doppler sensor designed using these impedance measurements and its use in a diplex Doppler system have been discussed.

References

[1] R. Brown, F. C. Monds, and J. A. C. Stewart, "Short-range solid-state diplex radars," in *Proc. 6th Colloqium on Microwave Communication*, Budapest, Hungary, 1978.

[2] J. S. Wight, O. P. Jain, W. J. Chudobiak, and V. Makios, "Equivalent circuits of microstrip impedance discontinuities and launchers," *IEEE Trans. Microwave Theory Tech.*, vol. MTT-22, pp. 48–52, Jan. 1974.

[3] I. J. Bahl, "Build microstrip antennas with paper thin dimensions," *Microwaves*, vol. 18, no. 10, pp. 50–63, Oct. 1979.

[4] J. R. East, H. Nguyen-Ba, and G. I. Haddad, "Design, fabrication, and evaluation of BARITT devices for doppler system applications," *IEEE Trans. Microwave Theory Tech.*, vol. MTT-24, pp. 943–948, Dec. 1976.

[5] S. P. Kwok, and K. P. Weller "Low-cost X-band MIC BARITT Doppler sensor," *IEEE Trans. Microwave Theory Tech.*, vol. MTT-27, no. 10, pp. 844–847 Oct. 1979.